Nigerian Journal of Technology (NIJOTECH)
Vol. 44, No. 2, June, 2025, pp.173 - 183
www.nijotech.com

Print ISSN: 0331-8443
Electronic ISSN: 2467-8821
https://doi.org/10.4314/njt.v44i2.1

APPLICATION OF VLASOV THEORY AND MULTI- VARIABLE POWER SERIES FOR ELASTIC STABILITY ANALYSIS OF MONO -SYMMETRIC BOX GIRDER

AUTHORS:
C. O. Ugwoke[1,*], M. E. Onyia[2], and O. A. Oguaghamba[3]

AFFILIATIONS:
[1,2,3]Department of Civil Engineering, University of Nigeria, Nsukka, Enugu State, Nigeria.

***CORRESPONDING AUTHOR:**
Email: calistusobinna2013@gmail.com

ARTICLE HISTORY:
Received: 01 October, 2024.
Revised: 26 May, 2025.
Accepted: 16 June, 2025.
Published: 07 July, 2025.

KEYWORDS:
Box Girder Bridge, Flexural, Distortional, Mono-Symmetric, Vlasov's theory, Power Series Approach, Clamped Supported. Multi-Variable Deformation.

ARTICLE INCLUDES:
Peer review

DATA AVAILABILITY:
On request from author(s)

EDITORS:
Chidozie Charles Nnaji

FUNDING:
None

Abstract

This study employs a combination of Vlasov's thin-walled beam theory and a multi-variable power series approach to analyze the elastic stability of mono-symmetric box girders, a class of thin-walled structural elements widely used in bridge engineering, subjected to eccentric transverse loading. The primary objective is to investigate the discrepancy between the shear center and the center of gravity, which induces complex coupled deformation modes, particularly flexural and distortional effects. Using Varbanov's modified generalized displacement functions, the governing differential equation of equilibrium were derived based on section properties evaluated at the pole and shear center, through a unit displacement approach. Essential cross-sectional parameters were obtained using enhanced product integrals (diagram multiplications). Given the complexity of the governing equation and boundary conditions, exact closed-form solutions were not attainable. To address this, three analytical methods, power series, trigonometric series, and Taylor-Maclaurin series, were applied to solve the reduced equations, enabling a comprehensive evaluation of flexural and distortional behaviors. Among these, the power series method proved most effective, accurately capturing the multi-variable interactions required to model realistic deformation patterns. Under eccentric loading, maximum flexural deformation occurred at 10 and 40 meters, while distortional deformation peaked at 40 meters and diminished near 45 meters. The Taylor-Maclaurin series showed maximum flexural deformation at 30 meters and distortional deformation at 9 meters. The trigonometric series revealed cyclic deformation patterns indicative of fluctuating load effects but lacked the precision needed for complex geometries. This study addresses a notable gap in the literature by providing a robust analytical framework for mono-symmetric girders and emphasizes the importance of advanced multi-variable analytical techniques in structural design and engineering education.

1.0 INTRODUCTION

Mono-symmetric box girders, a subclass of thin-walled structural members, are extensively employed in civil engineering applications, particularly in bridge construction, due to their favorable mechanical characteristics. Chief among these are their high strength-to-weight ratio and efficient resistance to flexural, torsional, and distortional deformations [1]. The inherent geometry of mono-symmetric box girders makes them especially suitable for structures with asymmetrical deck configurations, where eccentric loading is common, [2]. By optimizing material distribution, these girders can mitigate the adverse effects of eccentricity, offering improved structural behavior without substantially increasing

HOW TO CITE:
Ugwoke, C. O., Onyia, M. E., and Oguaghamba, O. A. "Application of Vlasov Theory and Multi- Variable Power Series for Elastic Stability Analysis of Mono-Symmetric Box Girder", *Nigerian Journal of Technology*, 2025; 44(2), pp. 173 – 183; https://doi.org/10.4314/njt.v44i2.1

material costs [1], [3]. Despite these advantages, the analytical modeling of mono-symmetric box girders presents significant challenges. The primary complexity arises from the misalignment between the shear center and the centroid (center of gravity), which introduces non-coincident axial and shear load paths.

This misalignment results in complex internal stress distributions and leads to elastic instability phenomena involving coupled deformation modes such as flexural-torsional, flexural-distortional, and combinations thereof [4], [5]. These coupled modes are difficult to analyze using conventional structural theories due to their inherent multi-dimensional interactions and the presence of warping deformations. Over the years, various theoretical models have been proposed to address these challenges, [6], [7], [8]. Early analytical techniques predominantly relied on trigonometric (Fourier) series expansions [1], which, although effective for simple geometries and boundary conditions, tend to suffer from slow convergence and increased computational cost for more complex configurations. Alternatively, Taylor–Maclaurin series methods have been utilized to improve accuracy in plate and shell stability analyses [9] and [10]. However, these methods become increasingly cumbersome when addressing multi-variable boundary value problems involving coupled deformation modes, as seen in thin-walled mono-symmetric profiles. Recognizing these limitations, recent research efforts have turned toward more sophisticated analytical formulations. In particular, Vlasov's thin-walled beam theory [7], which incorporates warping and non-uniform torsion has proven effective in capturing the behavior of thin-walled structures, especially when modified to account for cross-sectional asymmetry and warping effects, [11].

The study by [12], extended Vlasov's theory by integrating a power series approach to evaluate the flexural and distortional stability of mono-symmetric box girders with simply supported boundary conditions. This method demonstrated improved accuracy and convergence, especially for girders susceptible to coupled instabilities. Furthermore, recent work in beam theory has introduced novel formulations that account for shear deformation and warping effects. The study by [13] presented an analytical solution for the buckling of thick beams using a cubic polynomial shear deformation theory. While primarily focused on thick beams, the principles of this approach are relevant for extending thin-walled theory to cases where shear flexibility and warping interaction are non-negligible. In addition to these theoretical advancements, recent investigations into thin-walled stability analysis have emphasized the need for hybrid methods capable of handling complex geometries, mixed boundary conditions, and multi-cell configurations. For instance, a study by [14] introduced a modified variational principle for thin-walled box sections, which improved computational efficiency while maintaining accuracy for asymmetrical cross-sections. Similarly, [15], in their work, explored the influence of boundary-induced warping constraints on the stability of mono-symmetric steel box girders under lateral loading, highlighting the sensitivity of elastic critical loads to torsional-flexural interactions. Motivated by these gaps in the literature and the growing need for more versatile analytical tools, the present study proposes a hybrid analytical framework that combines the modified Vlasov thin-walled beam theory with a multi-variable power series expansion.

Unlike existing studies, this research focuses on mono-symmetric box girders subjected to transverse loading and incorporates clamped boundary conditions, an area that has received limited attention. The objective is to derive the governing differential equations for elastic stability under flexural and distortional deformation, formulate a suitable displacement function, and construct shape functions tailored for clamped end conditions. Subsequently, the study determines the critical load associated with flexural-distortional deformations using the obtained shape functions. This approach not only advances the theoretical modeling of mono-symmetric box girders but also provides a foundation for practical applications, such as improving design codes and enhancing engineering education in the field of thin-walled structure analysis. By integrating recent advancements and addressing unresolved analytical challenges, the present study contributes a novel and comprehensive method for assessing the elastic stability of complex box girder systems.

2.0 METHODOLOGY

The displacements in longitudinal ($U(x,s)$) and transverse ($V(x,s)$) directions for thin-walled closed structures under external torque are expressed as:

$$U(x,s) = \sum_{i=1}^{m} U_i(x)\varphi_i(s);\ V(x,s) = \sum_{k=1}^{n} V_K(x)\psi_K(s) \quad (1)$$

Where, x: Longitudinal coordinate along the axis of the structural member (e.g., beam or girder); s: Circumferential or perimeter coordinate along the closed cross-section of the thin-walled structure; m, n : Number of mode shapes (or basis functions) used in the approximation of $U(x,s)$ and $V(x,s)$, respectively; $U_i(x)$: Amplitude function (or modal

coordinate) in the longitudinal direction for the i[th] mode, a function that varies along the length of the member; $\varphi_i(s)$: Shape function (or mode shape) in the circumferential direction for the i[th] longitudinal displacement mode, captures how the displacement varies along the cross-section; V_k(x): Amplitude function for the k[th] transverse (or distortional) mode, also varies along the length x; $\psi_K(s)$: Transverse shape function for the k[th] mode, describes distortional variation along the perimeter of the cross-section.

The elastic direct and shear strain on and between the two planes, x and s are obtained as:

Direct Strain along the longitudinal direction, $\varepsilon_x(x,s)$:

$$\varepsilon_x(x,s) = \frac{\partial U(x,s)}{\partial x} = \sum_{i=1}^{m} U_i{}'(x)\varphi_i(s) \quad (2)$$

Direct Strain along the transverse direction, $\varepsilon_s(x,s)$:

$$\varepsilon_s(x,s) = \frac{\partial V(x,s)}{\partial s} = \sum_{k=1}^{n} V_K(x)\psi_K{}'(s) \quad (3)$$

Shear Strain between the transverse and longitudinal directions, $\gamma(x,s)$:

$$\gamma(x,s) = \frac{\partial U(x,s)}{\partial s} + \frac{\partial V(x,s)}{\partial x} = \sum_{i=1}^{m} U_i(x)\varphi_i'(s) + \sum_{k=1}^{n} V_k'(x)\Psi_k(s) \quad (4)$$

In similar approach, the direct elastic longitudinal and shear stresses associated with these strains are obtained as follows, $\sigma(x,s)$:

$$\sigma(x,s) = E\varepsilon_x(x,s) = E\frac{\partial U(x,s)}{\partial x} = E\sum_{i=1}^{m} U_i{}'(x)\varphi_i(s) \quad (5)$$

E: Young's modulus (modulus of elasticity), a measure of the material's stiffness under axial loading.

$$\tau(x,s) = G\gamma(x,s) = G\left(\sum_{i=1}^{m} U_i(x)\varphi_i'(s) + \sum_{k=1}^{n} V_k'(x)\Psi_k(s)\right) \quad (6)$$

G: Shear modulus**,** a measure of the material's stiffness under shear loading.

The strain energy U is derived using

$$\mathrm{U} = \frac{1}{2}\left[\int_L\int_S\left(\left(\frac{\sigma^2_{(X,S)}}{E} + \frac{\tau^2_{(X,S)}}{G}\right)t(s) + \frac{M^2(x,s)}{EI_s}\right)dxds\right] \quad (7)$$

Where, U: Total strain energy stored in the thin-walled closed section due to axial, shear, and bending effects; t(s): Wall thickness of the thin-walled section at location s along the perimeter; M(x,s): Bending moment at the location (x,s) on the structure; I_s or EI_s: Flexural rigidity at point s, where: I_s is the second moment of area about the axis of bending, EI_s is the product of Young's modulus and I_s, indicating resistance to bending; L: Total length of the structure (along the longitudinal axis x).

Expanding and simplifying $\sigma^2(x,s)$ and $\tau^2_{(x,s)}$using summation properties:

$$\sigma^2(x,s) = E^2\sum_{i=1}^{m} U'_{(X)}U_j'(x)\cdot\sum_{j=1}^{n}\varphi_i(s)\varphi_j(s) \quad (8)$$

$$\tau^2_{(x,s)} = \mathrm{G}^2\left(\sum_{i=1}^{m} U_i(x)\,U_j(x)\cdot\sum_{i=1}^{m}\varphi_i'(s)\varphi_j'(s) + \sum_{i=1}^{m} U_i(x)V_h'(x)\cdot\sum_{k=1}^{n}\varphi_i'(s)\Psi_h(s) + \sum_{k=1}^{n}\mathrm{U_j(x)}\,V_k'(x)\cdot\sum_{i=1}^{m}\varphi_j'(s)\,\Psi_k(s) + \sum_{k=1}^{n} V_h'(x)\,V_k'(\mathrm{x})\cdot\sum_{k=1}^{n}\Psi_h(s)\Psi_k(s)\right) \quad (9)$$

By applying the same technique to the moment expression:

$$M^2(x,s) = \sum_{k=1}^{n} M_k(s)M_h(s)\cdot\sum_{h=1}^{n} V_k(x)\,V_h(x) \quad (10)$$

Using the total work done by external loads, $\mathrm{W_E} = -q\int_L\int_S V(x,s)dxds$, the total potential energy becomes:

$$\Pi = \mathrm{U} + \mathrm{W_E} = \frac{1}{2}\left[\int_L\int_S\left(\left(\frac{\sigma^2_{(X,S)}}{E} + \frac{\tau^2_{(X,S)}}{G}\right) + \frac{M^2(x,s)}{EI_s}\right)t(s)dxds\right] - q\int_L\int_S V(x,s)dxds \quad (11)$$

q *or* q_h: external load

In simplifying form, substituting expansions for σ^2, τ^2, M^2, and strain energy contributions, Π becomes:

$$\Pi = \frac{1}{2}\left[\left(E\sum_{i=1}^{m} U_i'(x)U_j'(x)\cdot\sum_{j=1}^{n}\varphi_i(s)\varphi_j(s)\right)t(s)ds + \left(\mathrm{G}\left(\sum_{i=1}^{m} U_i(x)\,U_j(x)\cdot\sum_{i=1}^{m}\varphi_i'(s)\varphi_j'(s) + \sum_{i=1}^{m} U_i(x)V_h'(x)\cdot\sum_{k=1}^{n}\varphi_i'(s)\Psi_h(s) + \sum_{k=1}^{n}\mathrm{U_j(x)}\,V_k'(x)\cdot\sum_{i=1}^{m}\varphi_j'(s)\,\Psi_k(s) + \sum_{k=1}^{n} V_h'(x)\,V_k'(\mathrm{x})\cdot\sum_{k=1}^{n}\Psi_h(s)\Psi_k(s)\right)\right)t(s)ds + \frac{1}{EI_s}\sum_{k=1}^{m} M_k(s)M_h(s)\cdot\sum_{h=1}^{n} V_k(x)\,V_h(x)ds - \sum q_h V_h(x,s)\Big]dx \quad (12)$$

Where, $t(s)ds = dA$

Taking the limits, i, j, k and h as an integers 1,2,3,4 representing the modes of interaction, we have:

$$\sum_{j=1}^{n}\varphi_i(s)\varphi_j(s)\,dA = \int\varphi_i(s)\varphi_j(s)dA = a_{ij};\ \sum_{i=1}^{m}\varphi_i'(s)\varphi_j'(s)\,dA = \int\varphi_i'(s)\varphi_j'(s)dA = b_{ij};$$
$$\sum_{k=1}^{n}\varphi_i'(s)\Psi_h(s)dA = \int\varphi_i'(s)\psi_h(s)dA\,j = c_{hi};$$
$$\sum_{i=1}^{m}\varphi_j'(s)\,\Psi_k(s)dA = \int\varphi_j'(s)\psi_k(s)dA = c_{jk};$$
$$\sum_{k=1}^{n}\Psi_h(s)\Psi_k(s)dA = \int\psi_h(s)\psi_k(s) = r_{hk};\ \sum_{h=1}^{n}\frac{M_k(s)M_h(s)}{EI_{(s)}}dA = \frac{1}{E}\int\frac{M_k(s)M_h(s)}{EI_{(s)}} = s_{hk};$$
$$\sum q_h V_h(x,s) = \int q\psi_h ds = q_h \quad (13)$$

Thus, equation (12) becomes:

$$\Pi = \frac{E}{2}\sum a_{ij}U_i'(x)U_j'(x)dx + \frac{G}{2}\left[\sum b_{ij}U_i(x)U_j(x) + \sum c_{ih}U_i(x)V_h'(x)\right]dx + \frac{G}{2}\left[\sum c_{jk}U_j(x)V_k'(x) + \sum r_{hk}V_k'(x)V_h'(x)\right]dx + \frac{E}{2}\sum V_k(x)V_h(x)dx - \sum q_h V_h\mathrm{dx} \quad (14)$$

Therefore, equation (14) shows that the total potential energy Π is a functional of the form:

$$\Pi = F\left(U_iU_jV_kV_hU_i'U_j'V_k'V_h'\right) \quad (15)$$

Where, Π: Total potential energy of the system, which includes the internal strain energy minus the work done by external forces. In variational methods, this is minimized to obtain equilibrium equations; F(...): Represents a functional, a mapping from a set of functions (in this case, displacement fields and their

derivatives) to a scalar quantity (the total potential energy).

2.1 Governing Equation of Distortional Equilibrium of Box – Girder

The governing equations of distortional equilibrium for a box-girder are derived by minimizing the functional equation using the Euler-Lagrange technique in both the longitudinal and transverse directions. In the longitudinal direction, the equilibrium equation is

$$\frac{\partial F}{\partial U} - \frac{d}{dx}\left(\frac{\partial \pi}{\partial U_j'}\right) = 0 \quad (16)$$

In the transverse direction, it is

$$\frac{\partial F}{\partial V_h} - \frac{d}{dx}\left(\frac{\partial \pi}{\partial V_h'}\right) = 0 \quad (17)$$

Where, F_x is the first moment of area about $\bar{y} - axis$, F is the area of section material.

Carrying out the partial differential of equation (16) with respect to U_j, and equation (17) with respect to V_h, using Euler-Lagrange, we have:

$$\sum b_{ij}U_i(x) + \sum c_{kj}V_k'(x) - \frac{E}{G}\frac{d}{dx}\sum a_{ij}U_i'(x) = 0 \quad (18)$$

Where, $k = \frac{E}{G} = 2(1+\gamma)$, we have:

$$ka_{ij}\frac{d}{dx}\sum U_i'(x) - b_{ij}\sum U_i(x) - c_{kj}\sum V_k'(x) = 0 \quad (19)$$

$$c_{ih}\sum_{i=1}^{m} U_i'(x) + r_{kh}\sum_{k=1}^{n} V_k''(x) - ks_{hk}\sum_{h=1}^{n} V_k(x) + \frac{1}{G}\sum q_h = 0 \quad (20)$$

Taking the bounds of the variables i, j and k for i and j = 1,2,3 and k = 1,2,3,4 and the limits of the variables i, h and k for i = 1,2,3 and h, k = 1,2,3,4, and extending, [1], determined certain coefficients with zero values for mono-symmetrical cross-sections, emphasized the interaction of torsional- distortional, flexural-tortional, and flexural- distortional deformations, and highlighted the importance of non-trivial coefficients associated with deformation modes 2, 3 and 4.

$$\begin{bmatrix} a_{11}=0;\ a_{12}=a_{21}=0;a_{13}=a_{31}=0 \\ b_{11}=0;\ b_{12}=b_{21}=0;b_{13}=b_{31}=0 \\ c_{11}=0;\ c_{12}=c_{21}=0;\ c_{13}=c_{31}=0 \\ r_{11}=0;\ r_{12}=r_{21}=0;\ r_{13}=r_{31}=0 \\ s_{11}=0;\ s_{12}=s_{21}=0;s_{22}=0;\ s_{13}=s_{31}=0;\ s_{23}=s_{32}=0 \end{bmatrix} \quad (21)$$

According to [1], the relative coefficients for bending-deformation equilibrium are the coefficients for deformation modes 2 and 4. By replacing the irrelevant non-coefficients in the matrix equations obtained after the expansion of equations (19) and (20), while retaining the relative coefficient in equation (21), the governing differential equations (22) and (23) were obtained as follows:

$$V_4^{11} = K_1 \quad (22)$$

$$\epsilon_1 V_2^{IV} + \epsilon_2 V_4^{IV} - \beta_1 V_4^{11} = K_2 \quad (23)$$

Where, $\epsilon_1 = Ka_{22}c_{42};\ \epsilon_2 = Ka_{22}r_{44}; \beta_1 = (b_{22}r_{44} - c_{24}c_{42});$

$$K_1 = \left(\frac{c_{22}}{r_{24}c_{42} - c_{22}r_{44}}\right)\frac{q_4}{G} - \left(\frac{c_{42}}{r_{24}c_{42} - c_{22}r_{44}}\right)\frac{q_2}{G};\ K_2 = b_{22}\frac{q_4}{G} \quad (24)$$

Where, ϵ_1 is a deformation or strain-related parameter derived from the product of stiffness coefficient Ka_{22} and geometric or mode shape coefficient C_{42}; ϵ_2 is another strain-related term, also dependent on the same stiffness coefficient Ka_{22} and another geometric or mode shape term r_{44}; β_1 is a coefficient reflecting the interaction between bending stiffness b_{22}, and coupling terms C_{24} and C_{42}, likely indicating a mix of flexural and distortional behavior; $K_1$is a stiffness-related coefficient combining various geometric constants (C_{22} C_{42} r_{24} r_{44}) and generalized forces q^2, q^4, scaled by shear modulus G. It likely represents a component of deformation or internal force distribution; K_2 is another stiffness expression, combining a bending stiffness term b_{22}, generalized force q_4, and shear modulus G. It likely relates to flexural behavior.

2.2 Non-Dimensional Differential Equilibrium Equations

They are derived for deformation system (flexural-distortional), by expressing the longitudinal coordinate as a non-dimensional parameter within the structure's limits,

$$X = LR : 0 \le R \le 1 \quad (25)$$

Where, X is the directional coordinate of the thin-walled structure along the span, L; R is the corresponding non-dimensional surface or longitudinal dimension of the structure in the limits 0 to 1, [16].

Recall: $V_2^{iv}(x) = \frac{d^4V_2(x)}{dx^4};\ V_2''(x) = \frac{d^2V_2(x)}{dx^2}; V_4''(x) = \frac{d^2V_4(x)}{dx^2};$

$$V_4^{iv}(x) = \frac{d^4V_4(x)}{dx^3} \quad (26)$$

From Equation (25),

$$X = \mathrm{LR};\ \mathrm{dx} = \mathrm{LdR};\ \mathrm{dx^2} = (\mathrm{LdR})^2 = \mathrm{L^2dR^2};\ \mathrm{dx^4} = (\mathrm{LdR})^4 = \mathrm{L^4dR^4} \quad (27)$$

Substituting equation (27) into equations (22) and (23), we have:

$$\frac{d^2V_4(R)}{\mathrm{L^2dR^4}} = K_1 \quad (28)$$

$$\epsilon_1\frac{d^4V_2(R)}{\mathrm{L^4dR^4}} + \epsilon_2\frac{d^4V_4(R)}{\mathrm{L^4dR^4}} - \beta_1\frac{d^2V_4(R)}{\mathrm{L^2dR^2}} = K_2 \quad (29)$$

The solution to Vlasov's flexural-distortional equilibrium equations for a mono-symmetric box girder involves power series displacement functions. It emphasizes transverse deformation and its energy contribution through general solutions and boundary conditions.

2.3 Formulation of the Displacement Function in the Form of a Multi-Variable Power Series

The power series is a mathematical technique for solving differential equations by representing a function as an infinite sum of terms involving powers of a variable, [17]. It is particularly useful for linear ordinary differential equations, ODEs, allowing solutions to be expressed as power series expansions like;

$$w = w(x) = \sum_{m=0}^{\infty} \delta_m (x - x_0)^m = \delta_0 + \delta_1(x - x_0) + \delta_2(x - x_0)^2 + \delta_3(x - x_0)^3 + \delta_4(x - x_0)^4 + \delta_5(x - x_0)^5 + \delta_6(x - x_0)^6 + \delta_7(x - x_0)^7 + \delta_8(x - x_0)^8 + \ldots \quad (30)$$

Here, δ represents the polynomial, and e denotes the exponential function.

The function w(x) is expressed as a power series centered at x_0, with coefficients δ_m representing real or complex constants. If $x_0 = 0$, the series simplifies to a power series in powers of x, equation (31) and differentiation of this series up to the seventh and eighth times is discussed.

$$w = w(x) = \sum_{m=0}^{8} \delta_m x^m = (\delta_0 + \delta_1 x + \delta_2 x^2 + \delta_3 x^3 + \delta_4 x^4 + \delta_5 x^5 + \delta_6 x^6 + \delta_7 x^7 + \delta_8 x^8) \quad (31)$$

$$w^{V11} = 5040\delta_7 + 40320\,\delta_8 x + \ldots \sum_{m=7}^{\infty} m\,(m-6)\,\delta_m x^{m-7} \quad (32)$$

$$w^{V111} = 40320\delta_8 + \ldots \sum_{m=8}^{\infty} m\ \ (\mathrm{m} - 7)\delta_m x^{m-8} \quad (33)$$

Into the ordinary equation

$$(\delta_1 + 2\delta_2 x + 3\delta_3 x^2 + \cdots + 8\delta_8 x^7) - (\delta_0 + \delta_1 x + \delta_2 x^2 + \cdots + \delta_7 x^7) = 0 \quad (34)$$

Then we collect like powers of x, finding:

$$(\delta_1 - \delta_0) + (2\delta_2 - \delta_1)x + (3\delta_3 - \delta_2)x^2 + \ldots + (8\delta_8 - \delta_7)x^7 = 0 \quad (35)$$

Equating the coefficient of each power of x to zero, we have:

$$\delta_1 - \delta_0 = 0, 2\delta_2 - \delta_1 = 0, 3\delta_3 - \delta_2 = 0, \ldots 8\delta_8 - \delta_7 = 0 \quad (36)$$

Solving these equations, we may express $\delta_1, \delta_2, \delta_3, \delta_4 \ldots, \delta_8$ in terms of δ_0, which remains arbitrary:

$$\delta_1 = \delta_0, \delta_2 = \frac{\delta_1}{2} = \frac{\delta_0}{2!}, \delta_3 = \frac{\delta_2}{3} = \frac{\delta_0}{3!}, \delta_4 = \frac{\delta_3}{4} = \frac{\delta_0}{4!}, \ldots, \delta_8 = \frac{\delta_7}{8} = \frac{\delta_0}{8!} \quad (37)$$

$$40320\delta_8 - 5040\delta_7 = 0\ ,\ \ \delta_8 = \frac{\delta_7}{8} \quad (38)$$

With these values of the coefficients, the series solution becomes the known general solution, viz. general solution, That is,

$$w(x) = \delta_0 + \delta_0 x + \frac{\delta_0}{2!}x^2 + \cdots \frac{\delta_0}{8!}x^8 = \delta_o\left(1 + x + \frac{x^2}{2!} + \frac{x^3}{3!} + \frac{x^4}{4!} + \frac{x^5}{5!} + \frac{x^6}{6!} + \frac{x^7}{7!} + \frac{x^8}{8!}\right) = \delta_0 e^x \quad (39)$$

2.4 Extension of a Single-Variable Power Series to a Multi-Variable Finite Polynomial Displacement Function Incorporating Step Functions

The potential energy of a thin-walled box girder under flexural-distortional load is represented by the beam's transverse deformation "w," which can be expressed as a power series displacement function for clamped-clamped (CC) supported conditions.

STEP 1: Homogeneous Solution. From equation (39),

$$w(x) = \delta_0 e^x \quad (40)$$

Based on the binomial coefficients and theorem at a point where m = 8, we have:

$$(\delta + 1)^m = 1.\delta_0 + 8.\delta_0 + 28.\delta_0 + 56.\delta_0 + 70.\delta_0 + 56\,\delta_0 + 28\delta_0 + 8\delta_0 + \delta_0.1 = 0 \quad (41)$$

Then general solution of the homogenous ODE is represented as a finite polynomial in x with coefficients, $\delta_1, \delta_2, \delta_3, \ldots, \delta_8$, multiplied by the series expansion of e^x as follow:

$$w_h = (\delta_1 + \delta_2 x + \delta_3 x^2 + \delta_4 x^3 + \delta_5 x^4 + \delta_6 x^5 + \delta_7 x^6 + \delta_8 x^7)e^x \quad (42)$$

Therefore, in general, the logarithmic base (e), log. e^x is equal to Ine^x, where x > o. From the key properties of the natural logarithm, it follows that, $Ine^x = x$, hence, equation (42) becomes:

$$w_h = \delta_1 x + \delta_2 x^2 + \delta_3 x^3 + \delta_4 x^4 + \delta_5 x^5 + \delta_6 x^6 + \delta_7 x^7 + \delta_8 x^8 \quad (43)$$

Applying the properties of binomial expansion, we obtain;

$$(\delta + 1)^8 = \delta_1 x + \delta_2 x^2 + \delta_3 x^3 + \delta_4 x^4 + \delta_5 x^5 + \delta_6 x^6 + \delta_7 x^7 + \delta_8 x^8 \quad (44)$$

The binomial expansion of $(\delta+1)^8$ becomes binomial expansion coefficients similar to the sum of consecutive positive integers as follows:

$$1.\frac{\delta_1}{\delta_0} + 2.\frac{\delta_2}{\delta_1} + 3.\frac{\delta_3}{\delta_2} + 4.\frac{\delta_4}{\delta_3} + 5.\frac{\delta_5}{\delta_4} + 6.\frac{\delta_6}{\delta_5} + 7.\frac{\delta_7}{\delta_6} + 8.\frac{\delta_8}{\delta_7} \quad (45)$$

The hypothesis of equation (45) corresponds to the following expression:

$$\sum_{R=1}^{8} R.\frac{\delta_R}{\delta_{R-1}} = 1.\frac{\delta_1}{\delta_0} + 2.\frac{\delta_2}{\delta_1} + 3.\frac{\delta_3}{\delta_2} + 4.\frac{\delta_4}{\delta_3} + 5.\frac{\delta_5}{\delta_4} + 6.\frac{\delta_6}{\delta_5} + 7.\frac{\delta_7}{\delta_6} + 8.\frac{\delta_8}{\delta_7} \quad (46)$$

Where R = 1

Then, from the arithmetic series formula for the sum of consecutive integers, we obtained the following sum of the first 8 positive integers as follow:

$$\frac{[8(8+1)]}{2} = 36 \quad (47)$$

STEP 2: Particular Solution: From equation (39), let,

$$w_p = \delta_0 x^8 e^x \quad (48)$$

$$\begin{bmatrix} w_{p^I} = \delta_o(8x^7 + x^8)e^x \\ w_{p^{II}} = \delta_o(56x^6 + 16x^7 + x^8)e^x \\ w_{p^{III}} = \delta_o(336x^5 + 169x^6 + 24x^7 + x^8)e^x \\ w_{p^{Iv}} = \delta_o(1680x^4 + 1350x^5 + 337x^6 + 32x^7 + x^8)e^x \\ w_{p^{v}} = \delta_o(6720x^3 + 8430x^4 + 3372x^5 + 561x^6 + 40x^7 + x^8)e^x \\ w_{p^{vI}} = \delta_o(20160x^2 + 40440x^3 + 25290x^4 + 6738x^5 + 841x^6 + 48x^7 + x^8)e^x \\ w_{p^{vII}} = \delta_o(40320x + 141480x^2 + 141600x^3 + 58980x^4 + 11784x^5 + 1177x^6 + 56x^7 + x^8)e^x \\ w_{p^{vIII}} = \delta_o(40320 + 323280x + 566280x^2 + 377520x^3 + 117900x^4 + 18846x^5 + 1569x^6 + 64x^7 + x^8)e^x \end{bmatrix} \quad (49)$$

Here, equation (41), becomes;

$$1.\delta_0 + 8.\delta_0 + 28.\delta_0 + 56.\delta_0 + 70.\delta_0 + 56\,\delta_0 + 28\delta_0 + 8\delta_0 + \delta_0.1 = 36 \quad (50)$$

Substituting equation (49) into equation (50), gave:

$$(\delta_o(40320 + 323280x + 566280x^2 + 377520x^3 + 117900x^4 + 18846x^5 + 1569x^6 + \delta + 64x^7 + x^8) + 8_o(40320x + 141480x^2 + 141600x^3 + 58980x^4 + 11784x^5 + 6738x^5 + 841x^6 + 48x^7 + 70\delta_o(1680x^4 + 1350x^5 + 337x^6 + 32x^7 + x^8) + 56\delta_o(336x^5 + 169x^6 + 24x^7 + x^8 + 1177x^6 + x^8) + 56\delta_o(6720x^3 + 8430x^4 + 3372x^5 + 561x^6 + 40x^7 + x^8) + 56x^7 + x^8) + 28\delta_o(20160x^2 + 40440x^3 + 25290 + 28\delta_o(56x^6 + 16x^7 + x^8)x^4 + 8\delta_o(8x^7 + x^8) + \delta_o(x^8))e^x = 36 \quad (51)$$

Omitting the linear squares, the third, fourth, fiftieth, sixtieth, seventieth, and eightieth terms, and omitting the common factor, e^x, we obtain;

$$40320\delta_o = 36 \quad (52)$$

$$\delta_o = 8.9286 \times 10^{-4} \quad (53)$$

$$w_p = 8.9286 \times 10^{-4} x^8 e^x \quad (54)$$

STEP 3: Now, $w(x) = w_h + w_p$

$$w(x) = (\delta_1 + \delta_2 x + \delta_3 x^2 + \delta_4 x^3 + \delta_5 x^4 + \delta_6 x^5 + \delta_7 x^6 + \delta_8 x^7)e^x + 8.9286 \times 10^{-4} x^8 e^x \quad (55)$$

Equation (55) represents the generalized polynomial displacement function that accurately models the deformed shape of a thin-walled box girder under combined loads using Bentham's boundary conditions.

2.5 Derivation of Shape Functions for a Clamped (C) Supported Boundary Condition Using Power Series, Taylor–Maclaurin Series, and Trigonometric Series

Figure 1 illustrates the beam with clamped support conditions under various loads, where the displacement functions are expressed using power series, Taylor-Maclaurin series, and trigonometric series, with boundary conditions provided along the η-direction as follows:

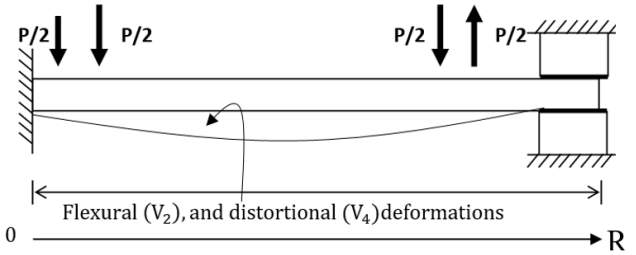

Figure 1: Clamped-Clamped (CC) supported beam along the R-axis, subjected to flexural-distortional loading, with superimposed results from power series, Taylor-Maclaurin series, and trigonometric series, showing boundary conditions along the R-direction

2.5.1 Power series shape function for CC beam

$w(R=0);\ w^{1R}(R=0)=0;\ w(R=1);\ w^{1R}(R=1)=0$

From equation (43)

$$w(R) = \Omega(R - 2R^3 + R^5) \quad (56)$$

Where, Ω is a proportionality constant, V_2(R) and V_4(R) are flexural and distortional deformations.

Hence, the corresponding equation of deformations, second and fourth order derivatives, becomes:

$$V_2(R) = \Omega_2(R - 2R^3 + R^5);\ V_4(R) = \Omega_4(R - 2R^3 + R^5) \quad (57)$$

$$V_2''(R) = \frac{d^2V_2}{dR^2}(R) = \Omega_2(-12R + 20R^3);\ V_2'^v(R) = \frac{d^4V_2}{dR^4}(R) = 120R$$

$$V_4''(R) = \frac{d^2V_4}{dR^2}(R) = \Omega_4(-12R + 20R^3);\ V_4'^v(R) = \frac{d^4V_4}{dR^4}(R) = 120R \quad (58)$$

2.5.2 Taylor Maclaurin's shape function for CC beam

By equating the moment and elasticity equations of beam and integrating twice with respect to an arbitrary direction η, the displacement function is obtained as:

$$W_\eta = C_o + C_1\eta \cdot + C_2\eta^2 + C_3 \cdot \eta^3 + C_4 \cdot \eta^4 \quad (59)$$

Where, C_o and C_1 are constants of integration, and $C_4 = \frac{q}{24D}$; $C_3 = \frac{-R}{6D}$; $C_2 = \frac{M_1}{2D}$. for a uniformly distributed load, the function is fourth-order, as the highest polynomial degree is 4. Thus, in the Taylor-Maclaurin series expansion for a beam strip along R, the maximum term is m = 4. The series constants along the R are denoted as A_m, [18,19, 20], thus,

$$w(R) = \sum_{m=1}^{\infty} A_m R^m \quad (60)$$

$$w(R) = \sum_{m=1}^{4} A_m R^m = (A_0 + A_1 R + A_2 R^2 + A_3 R^3 + A_4 R^4) \quad (61)$$

The coefficients A_m of the series are determined from the boundary conditions at the edges of the beam.

Boundary Conditions along η – direction

$$w(R=0);\ w^{1R}(R=0)=0; w(R=1);\ w^{1R}(R=1)=0 \quad (62)$$

From equation (62)

$$w(R) = \Omega(R^2 - 2R^3 + R^4) \quad (63)$$

Hence, the corresponding equation of deformations, second and fourth order derivatives, becomes:

$$V_2(R) = \Omega_2(R^2 - 2R^3 + R^4);\ V_4(R) = \Omega_4(R^2 - 2R^3 + R^4) \quad (64)$$

$$V_2''(R) = \frac{d^2V_2}{dR^2}(R) = \Omega_2(2 - 12R + 12R^2);\ V_2'^v(R) = \frac{d^4V_2}{dR^4}(R) = 24\Omega_2;$$

$$V_4''(R) = \frac{d^2V_4}{dR^4}(R) = \Omega_4(2 - 12R + 12R^2);\ V_4'^v(R) = \frac{d^4V_4}{dR^4}(R) = 24\Omega_4 \quad (65)$$

2.5.3 Trigonometric series displacement function for CC beam

Let the approximate displacement or shape function be,

$$w = 1 - \cos\left(\frac{2\pi R}{a}\right) \quad (66)$$

The corresponding first derivative of equation (66) becomes:

$$w^1 = \frac{2\pi}{a}\sin\left(\frac{2\pi R}{a}\right) \quad (67)$$

Boundary Conditions along η – direction becomes:

$$w(R=0);\ w^{1R}(R=0)=0; w(R=1);\ w^{1R}(R=1)=0 \quad (68)$$

Therefore, the assumed displacement functions satisfied the boundary conditions, therefore,

$$w(R) = \Omega\left(1-\cos\left(\frac{2\pi R}{a}\right)\right) \quad (69)$$

Hence, the corresponding equations of deformation, second and fourth order derivatives become:

$$V_2(R) = \Omega_2\left(1-\cos\left(\frac{2\pi R}{a}\right)\right); V_4(R) = \Omega_4\left(1-\cos\left(\frac{2\pi R}{a}\right)\right) \quad (70)$$

$$V_2''(R) = \frac{d^2V_2}{dR^2}(R) = \left(\frac{2\pi}{a}\right)^2\cos\left(\frac{2\pi R}{a}\right);\ V_2'^{v}(R) = \frac{d^4V_2}{dR^4}(R) = -\left(\frac{2\pi}{a}\right)^4\cos\left(\frac{2\pi R}{a}\right)$$
$$V_4''(R) = \frac{d^2V_2}{dR^2}(R) = \left(\frac{2\pi}{a}\right)^2\cos\left(\frac{2\pi R}{a}\right);\ V_4'^{v}(R) = \frac{d^4V_4}{dR^4}(R) = -\left(\frac{2\pi}{a}\right)^4\cos\left(\frac{2\pi R}{a}\right) \quad (71)$$

2.6 Application of Power Series Shape Function to Vlasov Theory on Flexural- Distortional of Mono-Symmetric Box Girder for Clamped Supported Ends

Substituting, the flexural and distortional deformations and their second and fourth order derivatives in Equations (57) and (58) into the governing differential equilibrium equation for thin – walled systems under flexural - distortional loads in Equations (28) and (29), and solving simultaneously we have:

$$\frac{d^2V_4(R)}{L^2dR^4} = k_1$$
$$\epsilon_1\frac{d^4V_2(R)}{L^4dR^4} + \epsilon_2\frac{d^4V_4(R)}{L^4dR^4} - \beta_1\frac{d^2V_4(R)}{L^2dR^2}) = k_2$$
$$\Omega_4\frac{(-12R+20R^3)}{L^2} = \mathrm{k}_1 \quad (72)$$
$$\Omega_4 = \frac{\mathrm{k}_1}{(-12R+20R^3)/L^2} \quad (73)$$

Substitute equation (73) into equation (29) to get Ω_2:

$$\Omega_2\frac{24}{L^4}\epsilon_1 + \Omega_4\frac{24\epsilon_2}{L^4} - \Omega_4\frac{\beta_1}{L^2}\Omega_4(-12R+20R^2) = k_2 \quad (74)$$
$$\Omega_2\frac{24}{L^4}\epsilon_1 + \Omega_4\left(\frac{24\epsilon_2}{L^4} - \frac{\beta_1}{L^2}(-12R+20R^3)\right) = k_2 \quad (75)$$

Using the equation (57), the flexural deformation $V_2(R)$ and the distortional deformation, $V_4(R)$, for the mono-symmetric box girder gave:

$$V_2(R) = \Omega_2(R-2R^3+R^5);\ V_4(R) = \Omega_4(R-2R^3+R^5)$$
$$V_2(R) = \mathrm{k}_2 - \frac{\frac{\mathrm{k}_1}{(-12R+20R^3)/L^2}\left(\frac{24\epsilon_2}{L^4} - \frac{\beta_1}{L^2}(-12R+20R^3)\right)}{24\epsilon_1/L^4}(R-2R^3+R^5) \quad (76)$$
$$V_4(R) = \frac{k_1}{(-12R+20R^3)/L^2}(R-2R^3+R^5) \quad (77)$$

2.7 Application of Taylor Maclaurin Polynomial Shape Function to Vlasov Theory on Flexural-Distortional of Mono-Symmetric Box Girder for Clamped Supported Ends

Substituting, the flexural and distortional deformations and their second and fourth order derivatives in Equations (64) and (65) into the governing differential equilibrium equation for thin – walled systems under flexural - ditortional loads in Equations (28) and (29) and solving simultaneously we have:

$$\Omega_4\frac{(2-12R+12R^2)}{L^2} = k_1 \quad (78)$$
$$\Omega_2\frac{24}{L^4}\epsilon_1 + \Omega_4\left(\frac{24\epsilon_2}{L^4} - \frac{\beta_1}{L^2}(2-12R+12R^2)\right) = k_2 \quad (79)$$

Certainly! Let's isolate Ω_2 and Ω_4 from equations (78) and (79)

Equation (29) involves only Ω_4, so the expression for Ω_4 is:

$$\Omega_4 = \frac{k_1}{(2-12R+12R^2)/L^2} \quad (80)$$

Substitute equation (80) into equation (79) to get Ω_2:

$$\Omega_2\frac{24}{L^4}\epsilon_1 + \frac{k_1}{(2.12R+12R^2)/L^2}\left(\frac{24\epsilon_2}{L^4} - \frac{\beta_1}{L^2}(2-12R+12R^2)\right) = k_2 \quad (81)$$
$$\Omega_2 = \frac{k_2 - \frac{k_1}{(2-12R+12R^2)/L^2}\left(\frac{24\epsilon_2}{L^4} - \frac{\beta_1}{L^2}(2-12R+12R^2)\right)}{24\epsilon_1/L^4} \quad (82)$$

Using the equation (64), the flexural deformation, $V_2(R)$ and the distortional deformation,$V_4(R)$, for the mono-symmetric box girder gave:

$$V_2(R) = \Omega_2(R^2-2R^3+R^4);\ V_4(R) = \Omega_4(R^2-2R^3+R^4)$$
$$V_2(R) = \frac{k_2 - \frac{k_1}{(2-12R+12R^2)/L^2}\left(\frac{24\epsilon_2}{L^4} - \frac{\beta_1}{L^2}(2-12R+12R^2)\right)}{24\epsilon_1/L^4}(R^2-2R^2+R^4) \quad (83)$$
$$V_4(R) = \frac{k_1}{(2-12R+12R^2)/L^2}(R^2-2R^3+R^4) \quad (84)$$

2.7 Application of Trigonometric Series Shape Function to Vlasov Theory on Flexural-Distortional of Mono-Symmetric Box Girder for Clamped Supported Ends

Substituting, the flexural and distortional deformations and their second and fourth order derivatives in Equations (70) and (71) into the governing differential equilibrium equation for thin – walled systems under flexural - distortional loads in Equations (28) and (29), and solving simultaneously we have:

$$\Omega_4\frac{1}{L^2}\left(\frac{2\pi}{a}\right)^2\cos\left(\frac{2\pi R}{a}\right) = \mathrm{k}_1 \quad (85)$$
$$\Omega_4 = \frac{\mathrm{k}_1}{\frac{1}{L^2}\left(\frac{2\pi}{a}\right)^2\cos\left(\frac{2\pi R}{a}\right)} \quad (86)$$

Equation (26):

$$\Omega_2 \frac{1}{L^4}\left(-\left(\frac{2\pi}{a}\right)^4 \cos\left(\frac{2\pi R}{a}\right)\right)\epsilon_1 + \Omega_4\left(\frac{1}{L^4}\left(-\left(\frac{2\pi}{a}\right)^4 \cos\left(\frac{2\pi R}{a}\right)\right)\epsilon_2 - \beta_1 \frac{1}{L^2}\left(\frac{2\pi}{a}\right)^2 \cos\left(\frac{2\pi R}{a}\right)\right) = k_2 \quad (87)$$

Substituting equation (86) into equation (87), we have:

$$\Omega_2 \frac{1}{L^4}\left(-\left(\frac{2\pi}{a}\right)^4 \cos\left(\frac{2\pi R}{a}\right)\right)\epsilon_1 + \frac{k_1}{\frac{1}{L^2}\left(\frac{2\pi}{a}\right)^2 \cos\left(\frac{2\pi R}{a}\right)}\left(\frac{1}{L^4}\left(-\left(\frac{2\pi}{a}\right)^4 \cos\left(\frac{2\pi R}{a}\right)\right)\epsilon_2 - \beta_1 \frac{1}{L^2}\left(\frac{2\pi}{a}\right)^2 \cos\left(\frac{2\pi R}{a}\right)\right) = k_2 \quad (88)$$

$$\Omega_2 = \frac{k_2 - \frac{k_1}{\frac{1}{L^2}\left(\frac{2\pi}{a}\right)^2 \cos\left(\frac{2\pi R}{a}\right)}\left(\frac{1}{L^4}\left(-\left(\frac{2\pi}{a}\right)^4 \cos\left(\frac{2\pi R}{a}\right)\right)\epsilon_2 - \beta_1 \frac{1}{L^2}\left(\frac{2\pi}{a}\right)^2 \cos\left(\frac{2\pi R}{a}\right)\right)}{\frac{1}{L^4}\left(-\left(\frac{2\pi}{a}\right)^4 \cos\left(\frac{2\pi R}{a}\right)\right)\epsilon_1} \quad (89)$$

Using the equation (73), the flexural deformation $V_2(R)$, and the distortional deformation, $V_4(R)$, for the mono-symmetric box girder gave:

$$V_2(R) = \Omega_2\left(1 - \cos\left(\frac{2\pi R}{a}\right)\right);\ V_4(R) = \Omega_4\left(1 - \cos\left(\frac{2\pi R}{a}\right)\right)$$

$$V_2(R) = \frac{k_2 - \frac{k_1}{\frac{1}{L^2}\left(\frac{2\pi}{a}\right)^2 \cos\left(\frac{2\pi R}{a}\right)}\left(\frac{1}{L^4}\left(-\left(\frac{2\pi}{a}\right)^4 \cos\left(\frac{2\pi R}{a}\right)\right)\epsilon_2 - \beta_1 \frac{1}{L^2}\left(\frac{2\pi}{a}\right)^2 \cos\left(\frac{2\pi R}{a}\right)\right)}{\frac{1}{L^4}\left(-\left(\frac{2\pi}{a}\right)^4 \cos\left(\frac{2\pi R}{a}\right)\right)\epsilon_1}\left(1 - \cos\left(\frac{2\pi R}{a}\right)\right) \quad (90)$$

$$V_4(R) = \frac{k_1}{\frac{1}{L^2}\left(\frac{2\pi}{a}\right)^2 \cos\left(\frac{2\pi R}{a}\right)}\left(1 - \cos\left(\frac{2\pi R}{a}\right)\right) \quad (91)$$

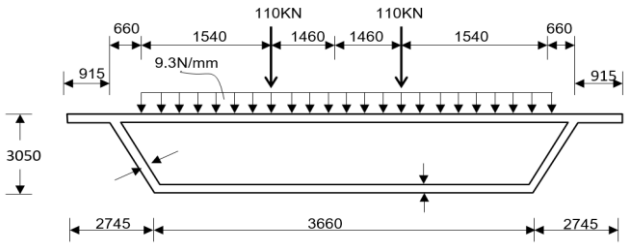

Figure 2: Mono-symmetric box girder. (The bridge is span 50m between piers)

3.0 RESULTS AND DISCUSSION

3.1 Numerical Mono–Symmetric Box Girder Bridge Problem

Consider a mono – symmetric box Girder Bridge of two – ways – two – lanes carrying a live load of 9.3N/mm (HL – 93 loading according to AASHTO), [21, 22,23], in addition to tandem double axle loads of 110KN each lane. The live load is uniformly distributed over the 7.32m transverse width of the bridge of two lanes – two – way. The loads are positioned at the outermost possible location to generate the maximum bending and distortional effect as shown in Figure 2.

3.2 Computation of Vlasov Coefficients

The Vlasov coefficients; a_{ij}, b_{ij}, c_{ij} and s_{kh} are obtained by multiplying, ϕ_i, ψ_i and M_k accordingly using the product integral for unit thickness (i.e; t = 1) as described by [24]. However, the modified product integral according to [25] is used, where the constant k value is unity, representing the thickness of the box girder, t.

3.3 Evaluation of the Flexural and Distortional Coefficients

$$\epsilon_1 = k_{a22}c_{42} = 2.5 \times 123.5117 \times 6.4170 = 1{,}981.446447 \quad (92)$$

$$\epsilon_2 = k_{a22}r_{44} = 2.5 \times 123.5117 \times 72.0033 = 22{,}233.12497 \quad (93)$$

$$\beta_1 = (b_{22}r_{44} - c_{22}c_{42}) = (14.6931 \times 72.0033 - 14.6931 \times 6.4170) = 963.6661 \quad (94)$$

$$k_1 = \left(\frac{c_{22}}{r_{24}c_{42} - c_{22}r_{44}}\right)\frac{q_4}{G} - \left(\frac{c_{42}}{r_{24}c_{42} - c_{22}r_{44}}\right)\frac{q_4}{G};\ k_1 = \left(\frac{14.6931}{6.4170 \times 6.4170 - 14.6931 \times 72.0033}\right)\frac{1.4738 \times 10^6}{9.6 \times 10^9} - \left(\frac{6.4170}{6.4170 \times 6.4170 - 14.6931 \times 72.0033}\right)\frac{1.0820 \times 10^6}{9.6 \times 10^9} = 114.4427732 \quad (95)$$

$$k_2 = b_{22}\frac{q_4}{G} = 14.6931 \times \left(\frac{1.4738 \times 10^6}{9.6 \times 10^9}\right) = 2.2556969556 \times 10^{-3} \quad (96)$$

3.4 Flexural and Distortional Deformations of Three Mathematical Tools or Series for Clamped Supported Ends

From equation (76) and (77) and determination of the associated Vlasov variables, the coefficients of the flexural and distortional deformations for the Power series are obtained as follows:

$$V_2(R) = 2.2556969556 \times 10^{-3} - \frac{114.4427732}{(-4.8 \times 10^{-3}R + 8 \times 10^{-3}R^3)}\frac{(0.085375199 - 0.38546644(-12R + 20R^3))}{7.608754356 \times 10^{-3}}$$

$$(R - 2R^3 + R^5) \quad (97)$$

$$V_4(R) = -\frac{114.4427732}{(-4.8 \times 10^{-3}R + 8 \times 10^{-3}R^3)}(R - 2R^3 + R^5) \quad (98)$$

From equation (83) and (84) and determination of the associated Vlasov variables, the coefficients of the flexural and distortional deformations for the Taylor Maclaurin's series are obtained as follows:

$$V_2(R) = \frac{2.2556969556 \times 10^{-3} - \frac{114.4427732}{(-12R + 12R^2)/50^2}\left(\frac{24 \times 22{,}233.12497}{50^4} - \frac{963.6661}{50^2}(2 - 12R + 12R^2)\right)}{24 \times 1{,}981.446447/50^4}(R^2 - 2R^2 + R^4) \quad (99)$$

$$V_4(R) = -\frac{114.4427732}{(8 \times 10^{-4} - 4.8 \times 10^{-3}R + 4.8 \times 10^{-3}R^2)}(R^2 - 2R^3 + R^4) \quad (100)$$

From equation (90) and (91) and determination of the associated Vlasov variables, the coefficients of the flexural and distortional deformations for the Trigonometric series are obtained as follows:

$$V_2(R) = -\frac{2.2556969556 \times 10^{-3} - \frac{114.4427732}{\frac{1}{50^2}\left(\frac{2\pi}{a}\right)^2 \cos\left(\frac{2\pi R}{a}\right)} \times \left(\frac{1}{50^4}\left(-\left(\frac{2\pi}{a}\right)^4 \cos\left(\frac{2\pi R}{a}\right)\right) \times 22{,}233.12497 - 0.38546644\left(\frac{2\pi}{a}\right)^2 \cos\left(\frac{2\pi R}{a}\right)\right)}{\frac{1}{50^4}\left(-\left(\frac{2\pi}{a}\right)^4 \cos\left(\frac{2\pi R}{a}\right)\right) \times 1{,}981.446447}$$

$$\left(1-\cos\left(\frac{2\pi R}{a}\right)\right) \quad (101)$$

$$V_4(R) = -\frac{114.4427732}{\frac{1}{50^2}\left(\frac{2\pi}{a}\right)^2\cos\left(\frac{2\pi R}{a}\right)}\left(1-\cos\left(\frac{2\pi R}{a}\right)\right) \quad (102)$$

3.5 Discussion of Results

This study examined the structural response of girders subjected to eccentric loading using three analytical modeling approaches: Power Series, Taylor Maclaurin Series, and Trigonometric Series. Each method was employed to evaluate deformation profiles, including both flexural and distortional effects along the girder span. The Power Series model demonstrated the highest spatial resolution, enabling it to accurately capture localized deformation behaviors, particularly in the mid-span region. Significant flexural deformation was observed between 10 m and 40 m, as shown in Figure 3, consistent with the distribution of maximum bending moments caused by eccentric axial and transverse loads. These results align with prior studies on thin-walled members under eccentric loading, which showed similar flexural amplification in continuous systems [26].

The distortional deformation, which increased from 5 m, peaked at around 40 m, and stabilized near 45 m, reflects a classic transition from active warping to restrained end behavior, as also reported by [27]. This validates the need for localized reinforcements, such as intermediate stiffeners, web thickening, or torsional bracing, especially in regions of curvature reversal or near supports in continuous systems. In contrast, the Taylor Maclaurin Series model, though less capable of resolving fine-scale behavior, provided useful insights into general deformation trends. Flexural peaks were recorded at 5 m, 30 m, and 45 m, with the maximum at midspan, which is typical of simply supported or two-span continuous girders under distributed loading [28]. A distortional peak at 9 m suggests a potential local stress concentration, possibly due to load introduction or cross-sectional discontinuities. This is consistent with experimental work on box girders with asymmetric web-flange interactions [29]. While this model lacks local resolution, its computational efficiency makes it suitable for early-stage assessments, sensitivity analyses, and design variant comparisons.

The Trigonometric Series model revealed sinusoidal deformation patterns, which are indicative of cyclic or dynamic influences such as moving loads, mechanical vibration, or wind-induced actions. Such behavior correlates with findings in fatigue-prone infrastructure, where oscillatory stress fields contribute to crack initiation and propagation [30]. Though the model lacks localized fidelity, it offers a valuable perspective for dynamic response estimation and fatigue assessment, particularly for long-span girders subject to recurring service loads. Compared to simply supported beams, which typically exhibit symmetric flexural behavior and zero moment at supports, the girders in this study, modeled as continuous or partially restrained, displayed asymmetric deformation patterns due to the influence of eccentric loading. Simply supported systems under eccentric loads may exhibit maximum deflection at midspan but lack the secondary warping behavior seen in continuous systems [31]. Similarly, in fixed-end conditions, the presence of end moments reduces midspan deflection and distributes internal forces more evenly, but increases the complexity of boundary-induced distortions [32].

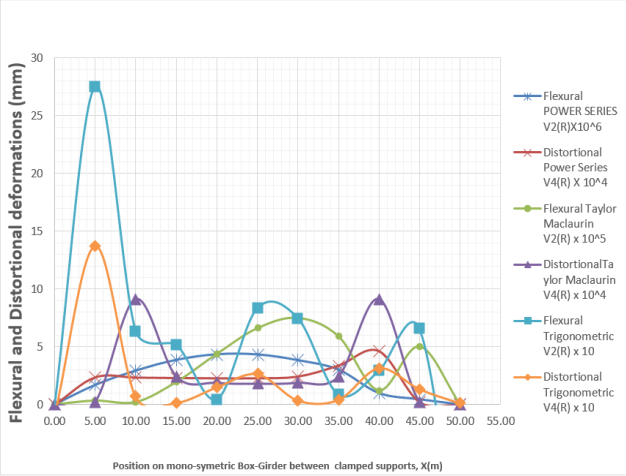

Figure 3: Flexural and distortional variation of a mono-symmetric box girder along the longitudinal span

The Power Series model captures these complex distributions more effectively than the other methods due to its multi-variable formulation and higher-order accuracy. Comparatively, the Power Series model, due to its robust formulation, is best suited for detailed structural evaluations under complex loading and boundary conditions. The Taylor Maclaurin and Trigonometric Series models, being single-variable, are more appropriate for preliminary designs, conceptual assessments, or screening studies. This mirrors standard engineering practice, where the analytical depth is adjusted according to the design phase and project complexity. The findings support an integrated modeling approach, combining both static and dynamic analyses, to gain a comprehensive understanding of girder behavior under eccentric loading. The practical implications of this study include optimized boundary condition selection such as partial fixity versus continuous support, use of

targeted reinforcements at midspan and near supports, incorporation of fatigue-resistant detailing, and consideration of vibration control measures for durability. Ultimately, model selection should be guided by a balance between accuracy, computational efficiency, and design objectives, aligning with the principles of performance-based and resilient infrastructure design.

4.0 CONCLUSIONS

The study examined a single-cell mono-symmetric box girder under flexural and distortional loads using various mathematical methods; Vlasov theory, power series, Taylor-Maclaurin, and trigonometric functions with clamped support conditions. The power series method outperformed the others by accurately modeling complex deformation and elastic stability, particularly under eccentric loading, due to its ability to incorporate multiple variables. In contrast, Taylor-Maclaurin and trigonometric functions, suitable for simpler beam analyses, lacked the precision needed for multi-dimensional behavior. While single-variable methods are helpful for preliminary insights, they oversimplify structural behavior and cannot capture the full range of interactions. Moreover, comparing multi-variable and single-variable approaches in civil engineering is inherently challenging due to their fundamental differences in scope and applicability. Overall, accurate analysis and design of mono-symmetric box girders require multi-variable methods like the power series to properly account for complex structural responses.

REFERENCES

[1] Osadebe, N. N., and Chidolue, C. A. "Flexural-distortional performance of thin-walled mono-symmetric box girder structures". *International Journal of Engineering Research & Technology*, 1(4), 1–9; 2012. ISSN 2278-0181. DOI n/a – URL available. ijert.org

[2] Wang, H., and Lee, J. "Modified Vlasov theory for non-symmetric thin-walled members". *Structural Engineering and Mechanics*, 56(4), 585-602; 2015. https://doi.org/10.12989/sem. 2015.56.4.585

[3] Nwokoye, O. S., Chidolue, C. A., and Ezeagu, C. A. "Effect of cross-sectional dimension on deformation of double-spine mono-symmetric box girder due to torsional-distortional loads". *Nnamdi Azikiwe University Journal of Civil Engineering*, 1(1), 98-120, 2023. DOI n/a – URL available. naujcve.com

[4] Zhao, C., Zhou, Y., Zhong, X., Wang, G., Yang, Q., and Hu, X. "A beam-type element for analyzing the eccentric load effect of box-girder bridges". *Structures*, 36, 1-12; 2022. https:// doi.org/10.1016/j.istruc.2021.11.001. sciencedirect.com

[5] Dahmani, L., Drizi, S., Djemai, M., Boudjemia, A., and Mechiche, M. O. "Lateral torsional buckling of an eccentrically loaded channel-section beam", *Strength of Materials*, 47(6), 912-916; 2015. https://doi.org/10.1007/s11223-015-9728-x researchgate.net

[6] Murray, N. W. "Introduction to thin-walled structures", (2nd ed.). *Oxford University Press*, 2022. ISBN 978-0-19-856715-2.

[7] Vlasov, V. Z. "Thin-walled space structures", (in Russian). Gosstrojizdat; 1958.

[8] Tesfaldet, G., and Vera, V. G. "The behaviour of thin-walled beams with restrained torsion", *Magazine of Civil Engineering*, 110(2), 2022. Article 11009. https://doi.org/10.34910/MCE. 110.9 researchgate.net

[9] Onyechere, I. C., Ibearugbulem, O. M., Anyaogu, U. C., and Awodiji, C. T. G. "Free-vibration study of thick rectangular plates using Taylor-Maclaurin polynomial displacement functions". *Saudi Journal of Engineering & Technology*, 5(2), 77-88; 2020. DOI n/a – journal URL.

[10] Huang, Y., and Li, Z. "Stability analysis of thin plates using Maclaurin-series solutions". *Thin-Walled Structures*, 46(4), 495-508; 2008. https://doi.org/10.1016/j.tws.2007.10.007

[11] Varbanov, C. P. "Theory of elasticity", (4th ed., pp. 254-271). *Technika Press*, Sofia, 1976.

[12] Ugwoke, C. O., Onyia, M. E., and Oguaghamba, O. A. "Evaluation of flexural and distortional elastic stability of mono-symmetric box girders with simply-supported conditions using Vlasov theory and a power-series approach", *Nigerian Journal of Technology*, 43(4), 610-617; 2024. https://doi.org/10.4314/ njt.v43i4.1 mail.nijotech.com

[13] Ike, C. C. "An analytical solution to buckling of thick beams based on a cubic-polynomial shear-deformation beam theory", *Engineering and Technology Journal*, 42(1), 90-103; 2024. https://doi.org/10.30684/etj.2023.142505.1538 academia.edu

[14] Zhang, Y., Liu, B., and Zhang, J. "Variational approach for stability of thin-walled box sections with warping constraints". *Thin-Walled Structures*, 187, 111189; 2023. https://doi.org/10.1016/j.tws.2023.111189

[15] Patel, R., and Kim, S. "Effect of warping boundary conditions on the stability of asymmetric box girders". *Journal of Bridge Engineering*, 28(6), 04023037; 2023. https://

doi.org/10.1061/(ASCE)BE.19435592.0001914

[16] Oguaghamba, O. A., Ezeh, J. C., Ibearugbulem, O. M., and Ettu, L. O. "Buckling and post-buckling load characteristics of all-edges-clamped thin rectangular plates". *International Journal of Engineering and Science*, 4(11), 55-61; 2015. DOI n/a – URL available.

[17] Kreyszig, E. "Advanced engineering mathematics", (10th ed., pp. 167-174). Wiley, 2011.

[18] Ezeh, J. C., Ibearugbulem, O. M., Nwadike, A. N., and Echehum, U. T. "Behaviour of buckled CSFS isotropic rectangular plates using a Taylor-Maclaurin polynomial-series shape function and the Ritz method". *International Journal of Engineering Science & Innovative Technology*, 3(1), 60-64; 2014. DOI n/a.

[19] Liu, J., Xiao, Y., and Liu, S. "Solutions to large beam-deflection problems by Taylor series and Padé approximants for compliant mechanisms", *Applied Mathematical Modelling*, 108, 37-54; 2022. https://doi.org/10.1016/j.apm.2022.02.015

[20] Öztürk, A. O., and Özer, H. "A spectral Taylor-polynomial solution of Euler-Bernoulli beam-vibration problems", *Journal of Düzce University*, 12(1), 32-45; 2023. DOI n/a.

[21] American Association of State Highway and Transportation Officials. "Interim revisions for LRFD steel-bridge design guide and material specifications", *AASHTO*, Washington, DC, 2023.

[22] Leahy, C., O'Brien, E. J., Enright, B., and Hajializadeh, D. "A review of the HL-93 bridge-traffic-load model using an extensive WIM database", *Proceedings of the ICE – Bridge Engineering*, 176(2), 136-154; 2023. https://doi.org/10.1680/jbren.22.00040

[23] California Department of Transportation. "Maximum moments and shears for HL-93 and P15 loads", (Bridge Design Memo 4-7). Caltrans, 2023.

[24] Rathore, A. K., and Kushwah, N. "A review on simulation analysis in lateral-torsional buckling of channel sections by ANSYS software". *International Journal of Trend in Scientific Research and Development*, 4(1), 687-696; 2019. https://doi.org/10.31142/ijtsrd25142.

[25] Bassetti, A., Ruggiero, S., and Candeloro, M. "Finite-element analysis of thin-walled structural elements using numerical integration". *International Journal of Structural Engineering*, 8(2), 104-118; 2017. https://doi.org/10.1504/IJSTRUCTE.2017.1000253.

[26] Zhao, L., and Helwig, T. A. "Design and behaviour of continuous steel box girders". *Journal of Structural Engineering*, 136(6), 654-664; 2010. https://doi.org/10.1061/(ASCE)ST.1943-541X.0000179

[27] Schafer, B. W., and Peköz, T. "Computational modelling of cold-formed steel: characterising geometric imperfections and residual stresses". *Journal of Constructional Steel Research*, 47(3), 193-210; 1998. https://doi.org/10.1016/S0143-974X(98)00004-8

[28] Timoshenko, S. P., and Gere, J. M. "Theory of elastic stability", (2nd ed.). McGraw-Hill, 1961.

[29] Bažant, Z. P., and Cedolin, L. "Stability of structures: Elastic, inelastic, fracture, and damage theories", (2nd ed.). World Scientific, 2010.

[30] Fisher, J. W., Yen, B. T., Klingerman, D. J., and Mertz, D. R. "Fatigue strength of steel beams with welded stiffeners and attachments", (NCHRP Report 147). Transportation Research Board, 1990.

[31] Mistry, M. A., and Sennah, K. T. "Distortional effects in steel box-girder bridges under eccentric loads". *Canadian Journal of Civil Engineering*, 33(7), 924-935; 2006. https://doi.org/ 10.1139/l06-045.

[32] Galambos, T. V. "Guide to stability design criteria for metal structures", (5th ed.). Wiley, 1998.